Available online at www.sciencedirect.com
ScienceDirect
Ceramics International 37 (2011) 3351–3355
CERAMICS INTERNATIONAL
www.elsevier.com/locate/ceramint

Synthesis and electrical properties of nanostructured $Ba_2SnYO_{5.5}$ proton conductor

Yanzhong Wang [a,b,*], Anthony Chesnaud [c], Emile Bevillon [b], Guilhem Dezanneau [b], Jinlong Yang [a]

[a] School of Materials Science and Engineering, North University of China, Taiyuan 030051, PR China
[b] Laboratoire Structure, Propriétés et Modélisation des Solides, Ecole Centrale Paris, Grande Voie des Vignes, 92295 Châtenay-Malabry Cedex, France
[c] Centre des Matériaux Pierre Marie Fourt, UMR CNRS 7633, Mines ParisTech, BP 87, 10 rue Henri Desbruères, 91003 Evry cedex, France

Received 14 March 2011; received in revised form 11 May 2011; accepted 25 May 2011
Available online 1 June 2011

Abstract

$Ba_2SnYO_{5.5}$ nanopowders were synthesized by a gel polymerization method. In this process, a gel containing Ba, Sn and Y cations has been obtained by the polymerization of acrylic acid using N,N′-methylene bis-acrylamide as a cross-linking reagent and hydrogen peroxide as an igniting reagent. The gel was calcined at 1200 °C, giving rise to the $Ba_2SnYO_{5.5}$ single-phase nanopowders with the grain size ranging from 50 nm to 70 nm. Nanopowders were sintered at 1150 °C by spark plasma sintering (SPS) to obtain dense nanostructure materials (> 95%) containing grains whose size ranges between 70 nm and 100 nm. Nanostructured $Ba_2SnYO_{5.5}$ shows a good chemical stability in wet atmosphere. However, its protonic conductivity decreases compared with that of microcrystallin $Ba_2SnYO_{5.5}$ ceramics.
© 2011 Elsevier Ltd and Techna Group S.r.l. All rights reserved.

Keywords: $Ba_2SnYO_{5.5}$; Nanostructure; Spark plasma sintering; Proton conduction

1. Introduction

Solid oxide fuel cells (SOFCs) currently require high operating temperature (> 800 °C) due to the low oxygen ion conductivity of the most electrolyte materials [1,2]. This hinders the wide applications of SOFCs in industry resulting from the accelerated thermal degradation and the use of expensive components. Proton conducting materials have attracted considerable interests due to the high conductivity at intermediate temperature. However, the development of proton conducting oxides appropriating for SOFCs is complicated by the conflict between high proton conductivity and chemical stability under the special atmosphere. For instance, the acceptor doped $BaCeO_3$ provide the highest proton conductivity, but it is not stable in the presence of high concentrations of CO_2-containing wet atmospheres below 600 °C [3–5]. Acceptor doped zirconates are very stable, but they show lower grain boundary conductivity than other ionic conductors [6]. Therefore, proton conductors that combine the high chemical stability of zirconates and high conductivity of cerates have attracted intensive attention [7].

$Ba_2SnYO_{5.5}$ compound belongs to the perovskite family and had been studied for their potential applications as electrolytes in SOFCs [8]. This compound provides high protonic conductivity comparable to that of $BaCeO_3$ based materials, and importantly it shows good chemical stability in CO_2-containing atmospheres. However, the structural instability was observed in the reduced and high water concentration atmosphere, which may be related to it high concentration of oxygen ions vacancies [8]. $Ba_2SnYO_{5.5}$ is usually synthesized by solid state reaction, which requires high calcination temperature (1000–1300 °C) to obtain a single phase and thus imposing the use of high sintering temperatures to reach good densification. For instance the relative density reaches only 85-95% while sintered at 1600–1700 °C [8]. Such a high temperature results in barium evaporation which leads to the decrease of proton conductivity.

Recently, a remarkable enhancement in the total ionic conductivity of about one order of magnitude has been found in nanostructured, heavily yttria- or samaria-substituted ceria ceramics compared with the conductivity of conventional

* Corresponding author at: School of Materials Science and Engineering, North Univeristy of China, Xueyuan Road 3, Taiyuan 030051, PR China. Tel.: +86 0351 3559638; fax: +86 0351 3559638.
E-mail address: wyzletter@hotmail.com (Y. Wang).

0272-8842/$36.00 © 2011 Elsevier Ltd and Techna Group S.r.l. All rights reserved.
doi:10.1016/j.ceramint.2011.05.135

microcrystallin ceramics [9], and the similar behaviours have also found in CeO_2–Gd_2O_3 and yttria-stabilized zirconia (YSZ) thin films [10,11]. The effect is attributed to the predominance of grain-boundary conduction in nanostructured materials, coupled with an increase in the grain-boundary ionic diffusivity with decreasing grain size [9,12].

The conductivity of microcrystallin $Ba_2SnYO_{5.5}$ ceramics has shown high proton conductivity in wet atmosphere. However, to our knowledge, the preparation, microstructure and protonic conductivity of dense and nanostructured $Ba_2SnYO_{5.5}$ have not been reported yet. In this work, we have prepared dense and nanostructured $Ba_2SnYO_{5.5}$ ceramics combining a gel polymerization method for nanopowders synthesis and spark plasma sintering (SPS) for dense nanostructured ceramics [13]. The evolutions of structure and microstructure of nanopowders with thermal treatment have been investigated by X-ray diffraction (XRD), Fourier transform infrared spectroscopy (FTIR) and scanning electron microscopy (SEM). The proton conductivities were investigated by A. C. impedance spectroscopy in dry and wet atmospheres.

2. Experimental

$Ba_2SnYO_{5.5}$ nanopowders were synthesized by a gel polymerization route from an aqueous solution containing cation salts, as described in ref. [14,15]. The precursor obtained was calcined at 900–1200 °C for 4 h to lead to the desired pure $Ba_2SnYO_{5.5}$ compounds.

For spark plasma sintering (SPS Dr Sinter 2080 furnace), 300–400 mg of powder was directly put into a cylindrical shaped graphite die in order to form final pellets of 8 mm in diameter and 1 mm of thickness. The die/powder assembly was then introduced into the sintering chamber. We observed that a sintering temperature of 1150 °C was sufficient to obtain good density. Nevertheless, Argon atmosphere was necessary (instead of vacuum) to avoid tin reduction. The sintering process is as followed: the pressure and temperature are progressively increased till their maximum (100 MPa and 1150 °C respectively), maintained during 1 min and then they are simultaneously released. Once the sintering process finished, a final thermal treatment of several hundreds of degrees is generally necessary to eliminate carbon pollution from the graphite die.

The phase formation of samples was investigated by X-ray powder diffraction (XRD, D5000, Siemens, Germany) using Cu $K_{\alpha 1+2}$ radiation partially filtered with a nickel foil to remove Cu K_β as X-ray source. The data were collected in the 2θ region from 20° to 60° in 2θ with 0.03° 2θ-step and 5 s/step. FTIR spectroscopy was performed on a Bruker IFS66 spectrometer in flowing nitrogen to detect the evolution of precursor phase with the temperature increase. The powders obtained were diluted in optically transparent KBr and pressed into pellets (the mass ratio of sample: KBr = 1:300). Various beam splitters and detectors were used to optimally cover the range from 4000 cm^{-1} to 100 cm^{-1}.

The microstructure of powders and pellets was characterized by scanning electron microscopy (Hitachi S-4700 SEM). The surface of samples was previously polished using SiC papers until the optical quality of surfaces were obtained, and then were thermally etched at 50 °C below the sintering temperature for 5 min with a heating scan of 2 °C min^{-1}. To allow their observation, a fine layer of gold metal was deposited onto the sample by radio frequency sputtering.

Electrical measurements were performed on a commercial sample-holder (Systems-Ionics) coupled to a Solartron 1260 frequency response analyzer. Acquisitions were performed at fixed temperatures after a stabilization of more than 1 h. The two sides of pellets were painted by platinum ink, dried at 100 °C in an oven, and further heat-treated at 1100 °C during 2 h. The measurements were carried out in dry and wet air atmospheres on the cooling starting from 800 °C to 150 °C, with a cooling rate of 200 °C/h for dry atmosphere and 50 °C/h for wet atmosphere. In the first case, drying was achieved by running the gas through a column of P_2O_5 desiccant, and humidification was obtained by bubbling gas through water.

3. Results and discussion

3.1. Structure of $Ba_2SnYO_{5.5}$ nanopowders and pellets

Fig. 1 shows XRD patterns of powders obtained after calcination in the temperature range from 700 °C to 1200 °C. The typical peaks of barium stannate were observed after thermal treatment at 700 °C for 4 h, although the residual impurity $BaCO_3$ with the main diffraction peak at 23.9° was detected until 1100 °C [16]. The intensity of the main peak of $BaCO_3$ decreases with increasing of calcination temperature, and is not further detected in the sample calcined at 1200 °C.

FTIR spectra of the precursors calcined at different temperatures are presented in Fig. 2. The band with absorption at 627 cm^{-1} is the characteristic stretching mode of Sn–O bonds [17]. Two absorption bands at 1443 cm^{-1} and 861 cm^{-1} correspond to $BaCO_3$ [18,19], and the intensity decreases with increasing temperature. However, this band is also detected after thermal treatment at 1200 °C, but it was not observed by X-ray diffraction measurements. Barium carbonate is difficult to remove completely at the low calcination temperature. It was

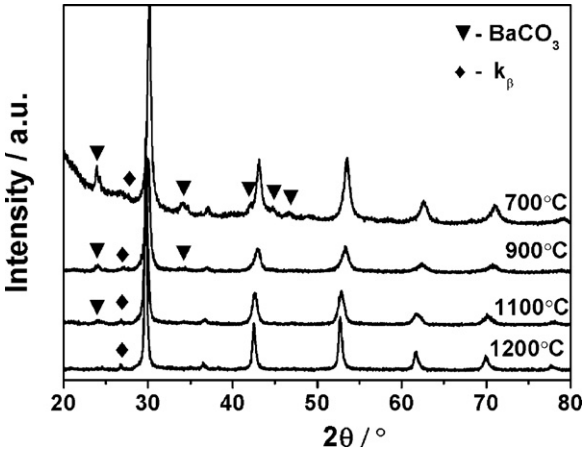

Fig. 1. X-ray diffraction patterns of gel-derived $Ba_2SnYO_{5.5}$ calcined at different temperatures for 4 h.

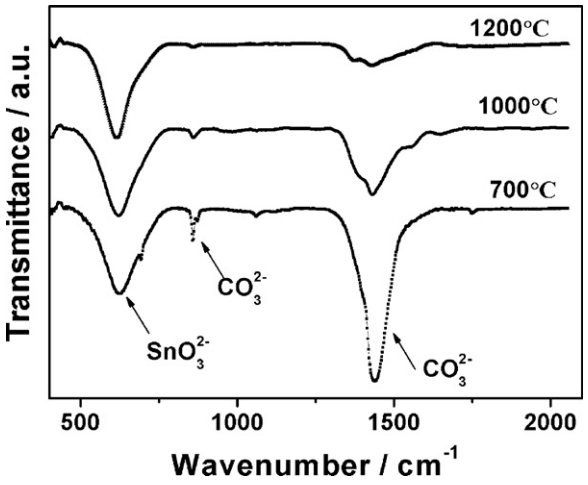

Fig. 2. FTIR Spectra of gel-derived $Ba_2SnYO_{5.5}$ treated at different temperatures for 4 h.

reported that the decomposition temperature of pure barium carbonate is above 1300 °C, and the $BaSnO_3$ phase was obtained at 1500 °C [16]. A. Sin et al. [20] reported that the precursor first calcined at 600 °C in oxygen atmosphere, and then at 1000 °C in argon atmosphere, which effectively removed $BaCO_3$. The persistence of carbonate peaks after treatment at high temperature could also be due to post-treatment surface carbonation of samples [20].

The morphology of powders calcined in the temperature range from 800 °C to 1200 °C is shown in Fig. 3. Regardless of calcination temperature, soft agglomerates are observed that contains almost cube-shaped particles. The average grain sizes are between 50 nm and 70 nm, and alter slightly with increasing of temperature. However, above 1100 °C, the distributions of grain size become very wide, and average grain size is in the range from 100 nm to 200 nm.

Fig. 4 shows the microstructure of samples. The dense ceramics were obtained by SPS at low temperature (1150 °C for 1 min), and the relative density is about 95%. However, it was reported that the relative density is only 85–95% while sintered at 1600–1700 °C using conventional sintering [8]. The average grain sizes of pellets measured in the SEM micrographs is about 70–80 nm. Comparing to the grain size of powders, it shows that the grains do not change during sintering by SPS.

3.2. Transport properties

Nyquist plots (Z' as real versus Z'' as imagine of the parametric function of frequency) for $Ba_2SnYO_{5.5}$ obtained at selected temperatures in wet and dry air atmospheres are displayed in Fig. 5. Below 500 °C, the impedance spectra consist in one depressed arc at high frequency (from 10^7 Hz to 10^2 Hz) that is attributed to the ceramic response, and a spike inclined at roughly 45°, at low frequency, that is attributed to the electrode response. The contributions of both bulk and grain boundaries can be identified and separated from least squares fitting of the impedance data, by using an equivalent electrical element consisting of a resistance in parallel with a constant phase element for each contribution [21]. However, above 500 °C, the characteristic frequency of the bulk response reaches a value higher than the maximum measurement

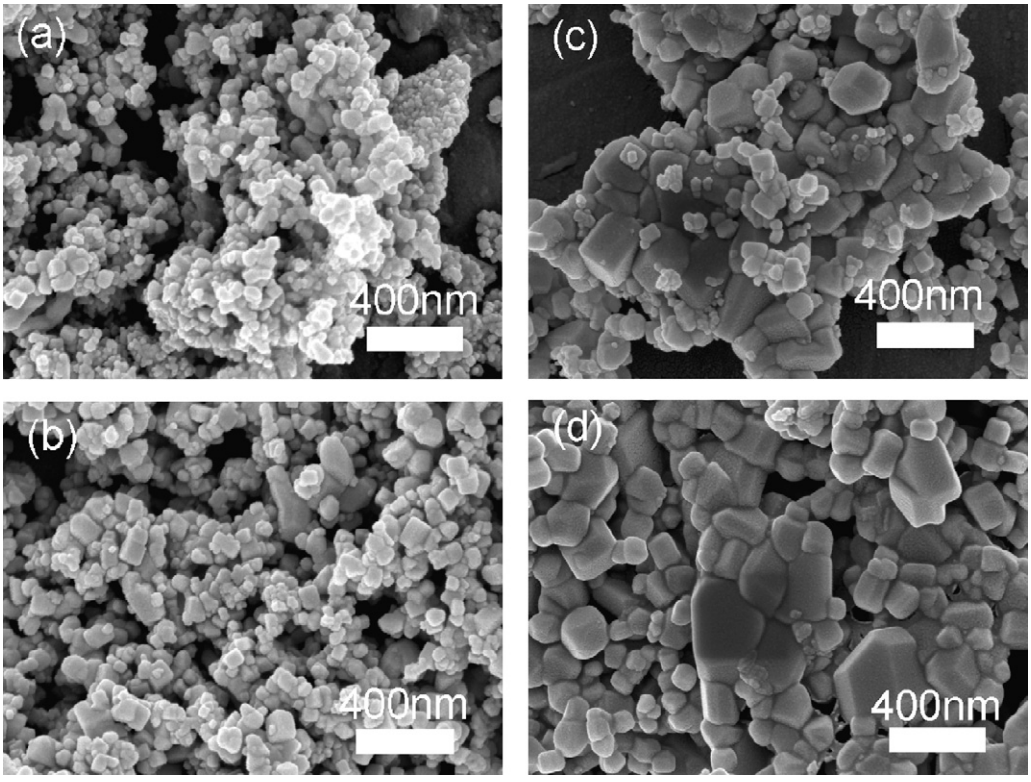

Fig. 3. SEM micrographs of $Ba_2SnYO_{5.5}$ powders: (a) 800 °C, (b) 1000 °C, (c) 1100 °C, (d) 1200 °C for 4 h.

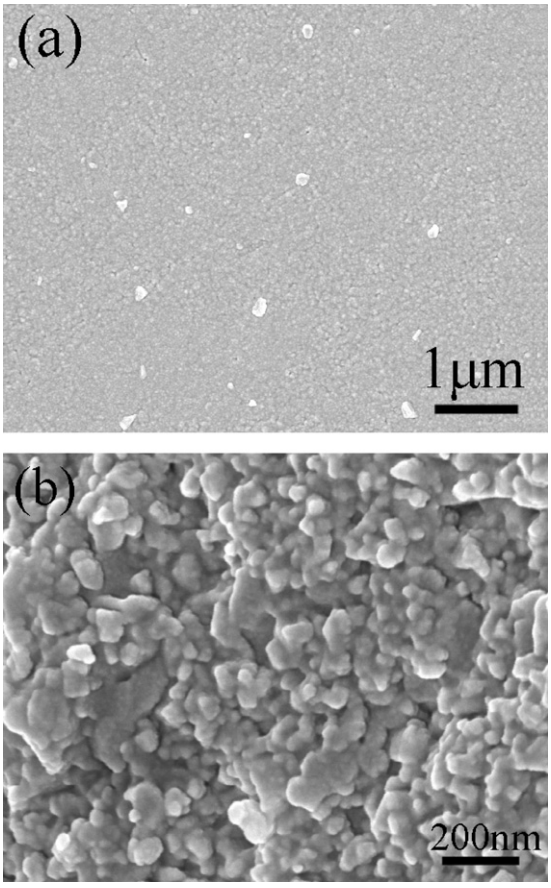

Fig. 4. SEM pictures of $Ba_2SnYO_{5.5}$ sintered by SPS at 1150 °C: (a) surface, (b) fracture.

frequency of the impedance meter and thus the bulk arc is not accessible [22].

The total, bulk and grain boundary conductivities are shown in Fig. 6. At low temperature, the total conductivity increased slightly when water is present in the system, and the activation energy of total conductivity is about 0.80 eV, which is much higher than that of $Ba_2SnYO_{5.5}$ (0.51 eV) prepared by solid state reaction [8]. The activation energy of bulk is about 0.44 eV, which is similar to the typical activation energies of proton conductors (0.40–0.50 eV) [23,24]. The total conductivity are nearly one order of magnitude lower than that of bulk conductivity in wet air, which indicates that the grain boundaries are the primary limitation to effective proton transport in these oxides, and the difference in bulk and grain boundary activation energies also supports this conclusion. In this study, an enhancement in the proton conductivity has not been found in nanostructured $Ba_2SnYO_{5.5}$. M.G. Bellino et al. reported that a transition from bulk-controlled to grain-boundary-controlled ionic conduction has been established when the average grain size of heavily substituted ceria is between 30 nm and 50 nm [9,12]. Concerning this point, the average grain size of nanostructured $Ba_2SnYO_{5.5}$ has not reached the critical grain size for the transition from bulk-controlled to grain-boundary-controlled proton conduction, and thus need further experiments to investigate the effect of smaller grain size on the proton conductivity in the future.

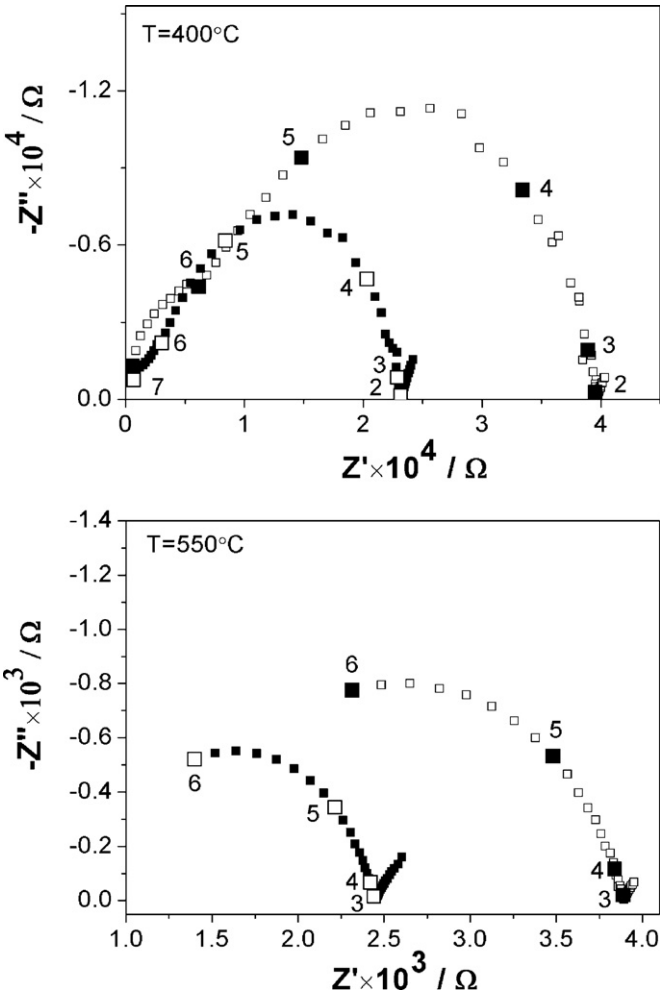

Fig. 5. The impedance spectra of $Ba_2SnYO_{5.5}$ sample in dry and wet air atmospheres at selected temperatures (solid square – wet air; open square – dry air).

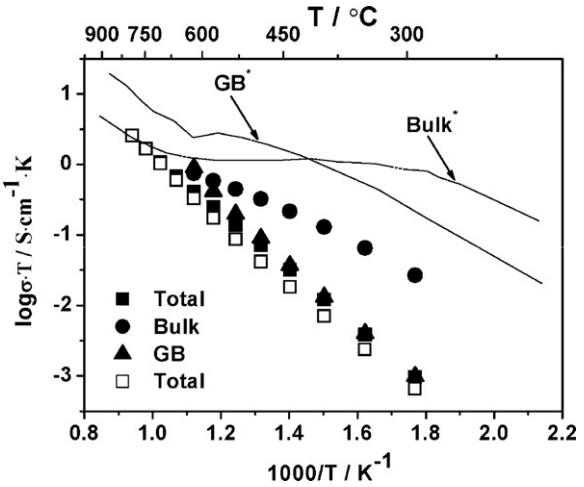

Fig. 6. The conductivities of $Ba_2SnYO_{5.5}$ sample under dry and wet air (solid: wet air; open: dry air). *The conductivity of bulk and grain boundary of $Ba_2SnYO_{5.5}$ [8] is given for comparison. The Measurement condition: $P_{H_2O} = 23\,\mathrm{hPa}(N_2)$.

4. Conclusions

$Ba_2SnYO_{5.5}$ nanopowders have been prepared by a gel polymerization method, and a single phase is formed at temperature above 1100 °C. The dense nanostructured ceramics (relative density > 95%) are obtained sintered at low temperature (1150 °C) by spark plasma sintering. The nanostructure of samples reduces the proton conductivity in wet atmosphere, and the total conductivity is one order of magnitude lower than that of the bulk conductivity in wet air, which results from the total conductivity is dominated by grain boundary resistance due to small grain size.

Acknowledgements

The study has been supported by the Agence Nationale de la Recherche through the NANOMATSOFC ''jeunes chercheurs'' project with number JC05_42231.

References

[1] N. Bonanos, K.S. Knight, B. Ellis, Perovskite solid electrolytes: structures, transport-properties and fuel cell applications, Solid State Ionics 79 (1995) 161–170.
[2] B.C.H. Steele, A. Heinzel, Materials for fuel cell technologies, Nature 414 (2001) 345–352.
[3] T. Yajima, H. Iwahara, H. Uchida, Protonic and oxide ionic conduction in $BaCeO_3$-based ceramics—effect of partial substitution for Ba in $BaCe_{0.9}O_{3-\delta}$ with Ca, Solid State Ionics 47 (1991) 117–124.
[4] J.F. Liu, A.S. Nowick, The incorporation and migration of protons in Nd-doped $BaCeO_3$, Solid State Ionics 50 (1992) 131–138.
[5] S.V. Bhide, A.V. Virkar, Stability of $BaCeO_3$-based proton conductors in water-containing atmospheres, J. Electrochem. Soc. 146 (1999) 2038–2044.
[6] F. Iguchi, N. Sata, T. Tsurui, Microstructures and grain boundary conductivity of $BaZr_{1-x}Y_xO_3$ ($x = 0.05$, 0.10, 0.15) ceramics, Solid State Ionics 178 (2007) 691–695.
[7] K.H. Ryu, S.M. Haile, Chemical stability and proton conductivity of doped $BaCeO_3$–$BaZrO_3$ solid solutions, Solid State Ionics 125 (1999) 355–367.
[8] P. Murugaraj, K.D. Kreuer, T. He, T. Schober, J. Maier, High proton conductivity in barium yttrium stannate $Ba_2YSnO_{5.5}$, Solid State Ionics 98 (1997) 1–6.
[9] M.G. Bellino, D.G. Lamas, N.E. Walsöe de Reca, Enhanced ionic conductivity in nanostructured, heavily doped ceria ceramics, Adv. Funct. Mater. 16 (2006) 107–113.
[10] I. Kosacki, T. Suzuki, V. Petrovsky, H.U. Anderson, Electrical conductivity of nanocrystalline ceria and zirconia thin films, Solid State Ionics 136–137 (2000) 1225–1233.
[11] T. Suzuki, I. Kosacki, H.U. Anderson, Microstructure-electrical conductivity relationships in nanocrystalline ceria thin films, Solid State Ionics 151 (2002) 111–121.
[12] M.G. Bellino, D.G. Lamas, N.E. Walsöe de Reca, A mechanism for the fast ionic transport in nanostructured oxide-ion solid electrolytes, Adv. Mater. 18 (2006) 3005–3009.
[13] A. Chesnaud, G. Dezanneau, C. Estournès, C. Bogicevic, F. Karolak, S. Geiger, G. Geneste, Influence of synthesis route and composition on electrical properties of $La_{9.33+x}Si_6O_{26+3x/2}$ oxy-apatite compounds, Solid State Ionics 179 (2008) 1929–1939.
[14] Y.Z. Wang, E. Bévillon, A. Chesnaud, G. Geneste, G. Dezanneau, Atomistic simulation of pure and doped $BaSnO_3$, J. Phys. Chem. C 47 (2009) 20486–20491.
[15] E. Bévillon, A. Chesnaud, Y.Z. Wang, G. Geneste, G. Dezanneau, Theoretical and experimental study of the structural, dynamical and dielectric properties of perovskite $BaSnO_3$, J. Phys.: Condens. Matter. 20 (2008) 145217.
[16] C.P. Udawatte, M. Kakihana, M. Yoshimura, Preparation of pure perovskite-type $BaSnO_3$ powders by the polymerized complex method at reduced temperature, Solid State Ionics 108 (1998) 23–30.
[17] W. Lu, H. Schmidt, Lyothermal synthesis of nanocrystalline $BaSnO_3$ powders, Ceram. Int. 34 (2008) 645–649.
[18] W. Lu, H. Schmidt, Hydrothermal synthesis of nanocrystalline $BaSnO_3$ using a $SnO_2{\cdot}xH_2O$ sol, J. Eur. Ceram. Soc. 25 (2005) 919–925.
[19] P. Durán, D. Gutierrez, J. Tartaj, M.A. Bañares, C. Moure, On the formation of an oxycarbonate intermediate phase in the synthesis of $BaTiO_3$ from (Ba,Ti)-polymeric organic precursors, J. Am. Ceram. Soc. 22 (2002) 797–807.
[20] A. Sin, B. Montaser, P. Odier, F. Weiss, Synthesis and sintering of large batches of barium zirconate nanopowders, J. Am. Ceram. Soc. 85 (2002) 1928–1932.
[21] R.C.T. Slade, S.D. Flint, N. Singh, Investigation of protonic conduction in Yb- and Y-doped barium zirconates, Solid State Ionics 82 (1995) 135–137.
[22] P. Babilo, S.M. Haile, Enhanced sintering of yttrium-doped barium zirconate by addition of ZnO, J. Am. Ceram. Soc. 88 (2005) 2362–2367.
[23] K.D. Kreuer, Proton-conducting oxides, Annu. Rev. Mater. Res. 33 (2003) 333–359.
[24] K.D. Kreuer, Aspects of the formation and mobility of protonic charge carriers and the stability of perovskite-type oxides, Solid State Ionics 125 (1999) 285–302.